ON THE GEOMETRICAL OPTIMIZATION OF CMOS HALL CELLS, RECTANGULAR AND SQUARE

Maria-Alexandra PAUN[1], Vladimir-Alexandru PAUN[2]

This paper presents geometrical optimization approaches, in order to improve the performances of the Hall cells. To this purpose, the geometrical correction factor was maximized, with respect to several imposed technological parameters, such as area and contacts size. The focus of this analysis is on both square and rectangular Hall structures, with small sensing contacts. Three-dimensional physical simulations for the square Hall cells are also included in this study. To complete the overview, experimental results regarding the sensitivity and offset of a certain square Hall cell, integrated in a CMOS technological process, are offered.

Keywords: Hall cells optimization, geometrical factor, contacts size, three-dimensional physical simulations

1. Introduction

The magnetic sensors based on Hall Effect have been used for decades and continue to be successfully employed nowadays in various applications in the industry, for current sensing, position measurement, in DC motors and in a myriad of low-power applications in the automotive industry [1-3]. Also, they have served various purposes in the biomedical engineering domains [4] and as magnetic cameras [5].

Due to the cost-effectiveness, robustness and easy integration on the chip, the CMOS technological process is preferred in the realization of the Hall Effect sensors. Both regular bulk [6] and SOI technological processes [7] have been used to fabricate these sensors.

The important parameters that govern the performance of such magnetic sensors are the sensitivity, offset and their temperature drift. An extensive investigation into the assessment of these parameters for CMOS Hall cells has been made by the first author in [6, 8]. To evaluate the performances of Hall cells

[1] PhD, Scientist, SCI STI CD, Ecole Polytechnique Fédérale de Lausanne (EPFL), CH-1015 Lausanne, Switzerland, Corresponding author: maria-alexandra.paun@epfl.ch
[2] PhD, Postdoctoral researcher, Computer Science and Systems Engineering Department, Ecole Nationale Superiore de Techniques Avancées (ENSTA), ParisTech, France, e-mail: paun@ensta.fr

in various technological processes and with different structures, both three-dimensional physical models [7] and circuit models have also been developed [9].

The approach of the geometrical correction maximization was initiated and studied by the first author in a paper from 2010, published in the Scientific Bulletin of UPB [10]. By staying in the same technological process, the geometrical correction factor should be maximized in order to guarantee the highest sensitivity. In the above-mentioned paper, this methodology has been proposed and thoroughly analyzed for the first time in great details over an array of eight different Hall shapes.

Essentially, the present paper continues the scientific research carried out and presented there. Also, we mention that the article under discussion has been very beneficial for the Hall designer communities and raised a lot of interest translated in the high number of 20 citations. This paper presents geometrical optimization procedures proposed for the Hall cells performance improvement, with an emphasis on square and rectangular structures with small contacts respectively.

The structure of the article, which is spanning over five chapters, is as follows. The second chapter talks about the geometrical correction factor, by introducing its definition for particular Hall structures. Still here, the geometrical correction factor maximization under technological and design constraints is performed, for rectangular Hall cells with small sensing contacts. Plots of the maximum geometrical correction factor with respect to the area and contacts sizes respectively are provided. The third chapter is devoted to the presentation of three-dimensional physical models for the square Hall cells. In Chapter 4, experimental results for the Square Hall cell integrated in a regular bulk 0.35 μm CMOS technological process are included, with an emphasis on sensitivity and offset. The paper finally concludes in Chapter 5.

2. Geometrical optimization

This section focuses on presenting the geometrical optimization considerations for Hall cells, with an emphasis on rectangular structures with small sensing contacts. More details about the present equations (theory, definitions, etc.) can be found in first author's PhD thesis [11] and paper [10], the latter cited by Udo Ausserlechner in 2016 [12] in the Scientific Bulletin of UPB.

A. Geometrical correction factor general definition

The geometrical correction factor G_H or simply G (*in extenso* "geometrical factor of Hall voltage") can be introduced in various ways, but in this context we prefer the classic formulation. According to the definition in Eq. (1), the

geometrical factor describes the diminution of the Hall voltage in a finite-size Hall device compared to that of a corresponding infinitely long device.

This diminution comes due to a non-perfect current confinement in Hall devices of finite dimensions. If the Hall voltage of an actual device is V_H, and $V_{H\infty}$ that of a corresponding infinitely long or point-contact device, the Hall geometrical factor is defined by:

$$G = \frac{V_H}{V_{H\infty}} \tag{1}$$

B. Square cells with contacts in the corners

We shall now consider a square structure with finite contacts of equal length situated in the corners of each side, and four axes of symmetry. This geometry is depicted in Figure 1.

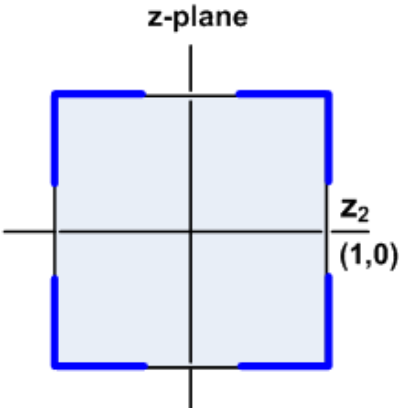

Fig. 1. The Square Hall cell with contacts in the corners

For this particular structure, the geometrical correction factor G is defined as it follows:

$$G = 1 - 1.094 m \operatorname{cotan}(\theta_H)\lambda^2,\ \lambda \to 0 \tag{2}$$

where θ_H is the Hall angle, while λ and m are defined below.

The parameter λ denotes the ratio between the sum of the lengths of the contacts c and the length of the boundary b:

$$\lambda = \frac{c}{b} \tag{3}$$

Further on, m is defined through the Hall angle θ_H with the aid of the formula:

$$\theta_H = \frac{m\pi}{2} = \arctan(\mu B) \tag{4}$$

By consequence, m is introduced as follows:

$$m = \frac{2\theta_H}{\pi} \tag{5}$$

For the square structure in Figure 1, the three-dimensional representation of the inverse of the geometrical correction factor G versus m and λ is illustrated in Figure 2.

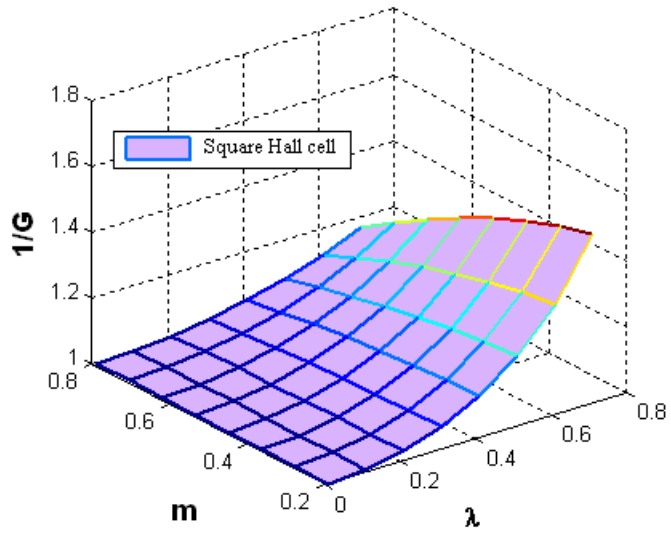

Fig. 2. The inverse of the geometrical correction factor 1/G, *versus* m and λ, for square Hall cells with contacts in the corners

C. Geometrical correction factor G maximization under technological and design constraints

If we include the length of the sensing contacts, we obtain the following simplified expression for the geometrical correction factor:

$$G = \left(1 - e^{-\frac{\pi L}{2W}}\left(1 - \frac{2}{\pi}\frac{s}{W}\right)\right) \tag{6}$$

which is valid if the length to width ratio L/W >1.5 and its sensing contacts are relatively small, namely s/W < 0.18.

In order to achieve maximum sensitivity, a geometrical correction factor G maximization was performed for rectangular Hall structures with small sensing contacts s. G was maximized when design specifications act as constraints, such as imposed sensing contacts length s and area $A=LW$.

To maximize the sensitivity for long Hall plates (L/W>1.5) with small sensing contacts, the cells dimensions can be chosen in such a way to guarantee a maximum G. The following graphs in Figures 3 and 4 represent the variation of W and L respectively with respect to the imposed area A, for different sensing contacts s. In this analysis, according to pertinent values related to the

technological process and optimized geometrical dimensions, we have considered the area A between 400 and 2500 µm^2 and the sensing contacts size s between 0.35 and 2 µm.

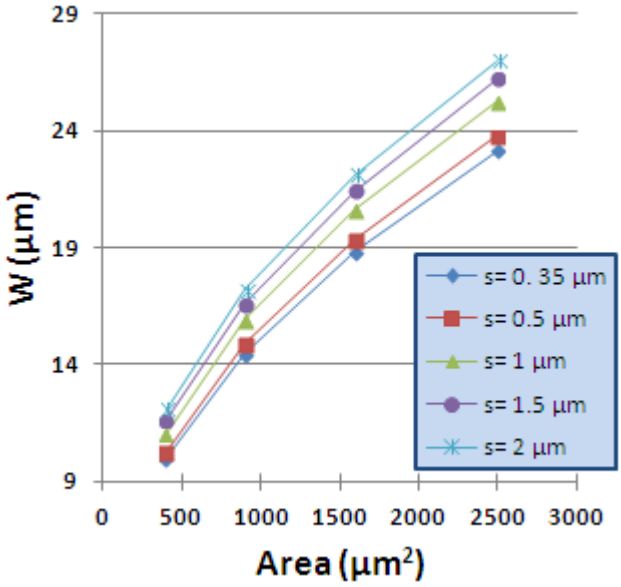

Fig. 3. Variation of W with respect to the imposed area, for different small sensing contact sizes, s

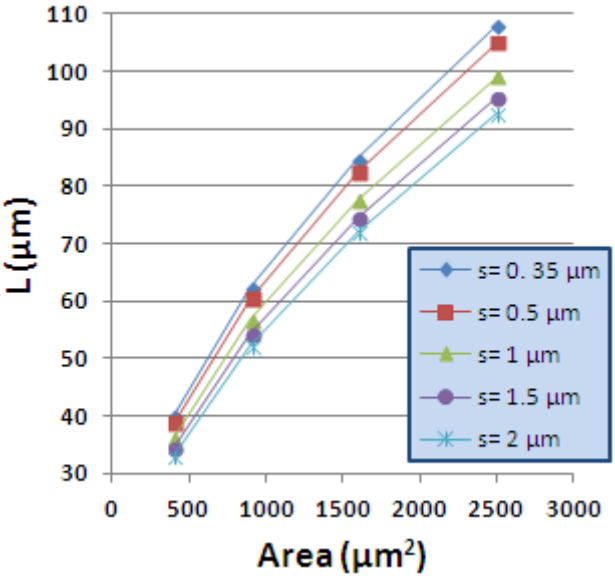

Fig. 4. Variation of L with respect to the imposed area, for different small sensing contact sizes, s

Figure 5 displays the variation of the maximum correction factor with respect to the imposed area A, for different small sensing contacts s. Hence, we

can infer that the geometrical correction factor *G* is maximum for the smallest contacts size *s* and the maximum area *A*.

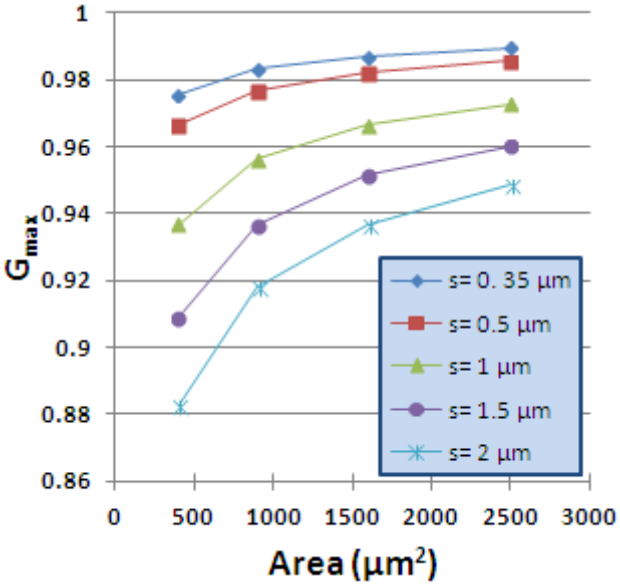

Fig. 5. Variation of maximum geometrical correction factor G_{max} with respect to the imposed areas *A*, for different small sensing contact sizes *s*

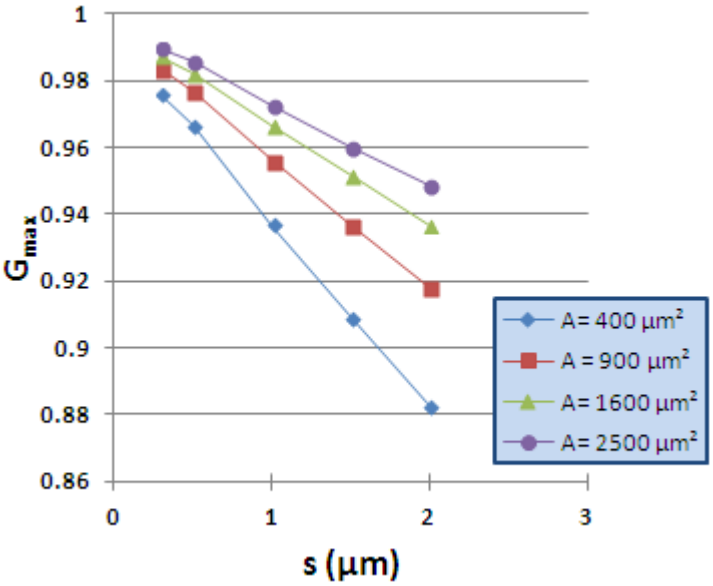

Fig. 6. Variation of maximum geometrical correction factor G_{max} with respect to the imposed sensing contact sizes *s*, for different imposed areas *A*

In Figure 6, the variation of the maximum correction factor *G* with respect to small sensing contacts *s*, for different imposed areas *A*, is represented. Again,

we can see that the maximum geometrical correction factor *G* is obtained for maximum area *A* and minimum contacts size *s*.

3. Three-dimensional physical simulations

An important tool in the verification of Hall cells performance and extraction of valuable information regarding the parameters of interest are the three-dimensional physical simulations.

Physical models of Hall cells in three-dimensions were developed using the Synopsys Sentaurus® TCAD software [13]. This solves the Poisson equation, electrons and holes continuity equations. In this way, for the semiconductor magnetic sensor, a numerical model in three-dimensions of the carrier transport process under the magnetic field influence is proposed, providing an insight into the current distribution and electrostatic potential. In order to model the carrier transport in magnetic field and to furthermore properly investigate the Hall voltage generation, the magnetic field acting on the semiconductor is provided through the galvanic transport model. The numerical simulations presented in this paper have been obtained using the Sentaurus tool.

A. Square Hall cell physical model

The Square Hall cell was modeled after a real CMOS 0.35 µm technological process, on a Silicon p-substrate (blue color) with an n-well active region (red color). The four electrical contacts, denoted from "*a*" to "*d*" and situated in the corners of the structure, are depicted in pink color.

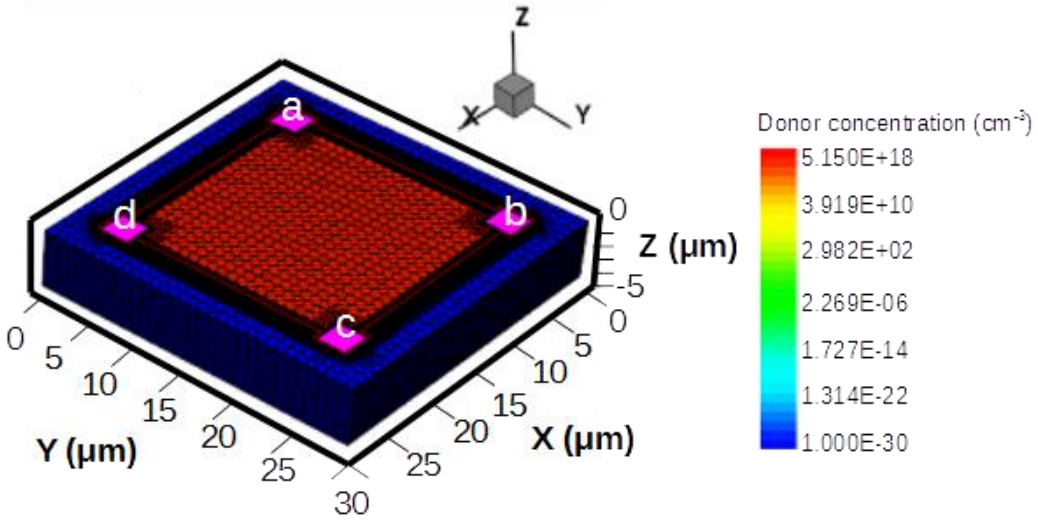

Fig. 7. Three-dimensional physical model of the Square Hall cell, depicting the donor concentration

In Figure 7, one could see the three-dimensional meshed structure of the Square Hall cell. The number of around 100'000 points in the meshed structure was optimized in order to allow for optimum accuracy and simulation run time.

Therefore, a p-substrate with a Boron concentration of 10^{+15} cm^{-3} and an active n-well region doped with Arsenic (peak concentration of $1.5 \cdot 10^{+17}$ cm^{-3}, Gaussian profile implantation) were used. This doping profile allows an average mobility of 630 $cm^2V^{-1}s^{-1}$ at the surface of the devices. Additional n+ regions were used for the contacts with n+ $=10^{+19}$ cm^{-3}. The donor concentrations in the Square Hall cell can also be seen in Figure 7.

B. Electrostatic potential of the Square Hall cell

Figure 8 presents the electrostatic potential distribution (color coded map) of the Square Hall cell. The structure was biased with 1 V on the "*a"* contact (red zone) and therefore a current was forced to flow between "*a*" and "*c*" contacts. As we can see, the electrical carriers deviate under the action of the Lorentz Force, through the influence of the magnetic field at specific strength B=0.5 T.

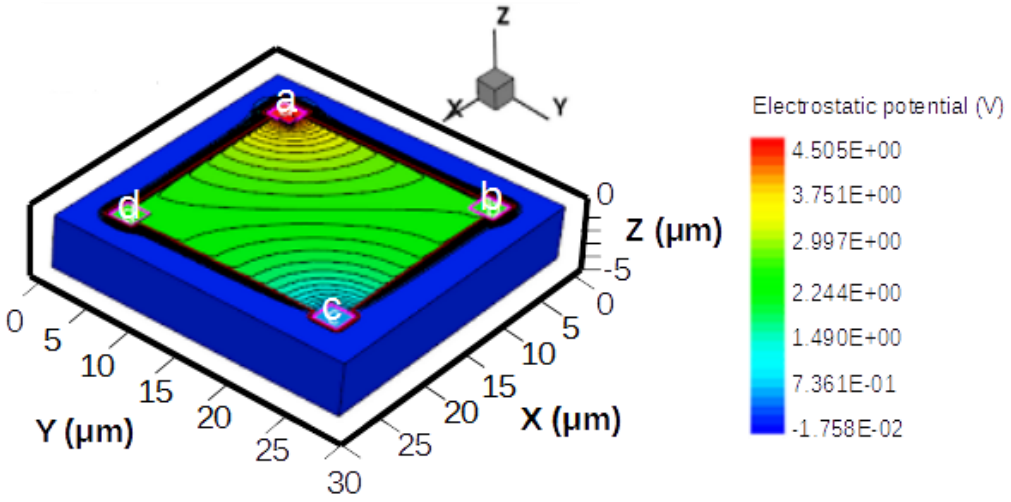

Fig. 8. Electrostatic potential for the Square Hall cell

As an observation, we have to mention that the three-dimensional physical simulations, Figure 7 and Figure 8 respectively, belong to the authors, through the improvement (geometrical structure definition, number of points, mesh refinement windows definition and placement, code running time optimization) of consecrated software.

4. Experimental results for Square Hall cells

This section introduces experimental results regarding the Square Hall cell, integrated in a CMOS 0.35 µm process, by providing an insight in the offset and sensitivity numerical values. The study will now focus on the Square Hall cell, of the type presented in Figure 1, and whose physical model was studied in the previous section.

As demonstrated in Section II, small contacts could increase the sensitivity. In this way, a good sensitivity was targeted with a non-cross cell, in the shape of the square cell with small contacts, which are located close to the borders of the p-n junction.

A. Square Hall cell sensitivity measurements

One of the most important parameters of Hall cells is the sensitivity, which is defined as the change in the output arising from a change in the input. Analytically, the absolute sensitivity S_A of Hall cells is defined as follows:

$$S_A = \left|\frac{V_{HALL}}{B}\right| = \frac{Gr_H}{nqt} I_{bias} \tag{7}$$

where B is the magnetic field induction, G is the geometrical correction factor, I_{bias} is the biasing current, r_H is the Hall scattering factor, n is the carrier density and t is the thickness of the active region [1]. In the case of silicon, the Hall scattering factor is usually 1.15.

In Figure 9, the absolute sensitivity of the Square Hall cell, both measured and simulated values, is depicted against a biasing current between 0 and 1 mA.

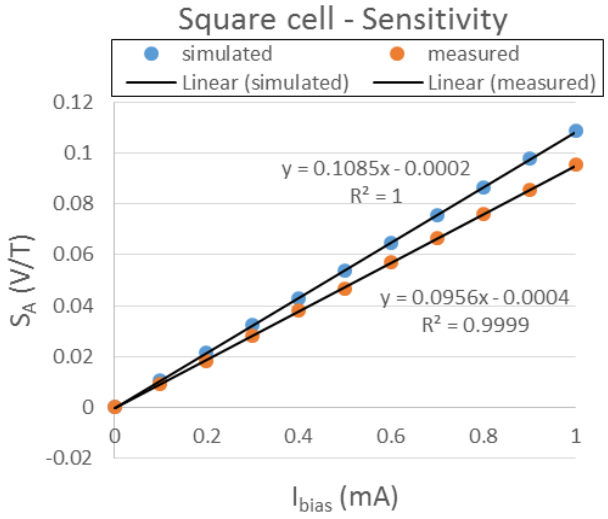

Fig. 9. Simulated absolute sensitivity S_A *vs.* biasing current, for the Square Hall cell

By looking at the results obtained in Figure 9, we can see that the absolute sensitivity at 1 mA is 108.54 mV (measured value), while the simulated value is 95.2 mV. The small discrepancies between the simulated and measured values are due to the fact that the real technological process parameters could not be exactly entirely reproduced in the simulator, due to the undisclosed nature of these parameters (implantation concentration, profile depth, etc.). However, further refinements in the simulation models are envisaged for future publications.

B. Square Hall cell offset measurements

The performance of the Hall cells is greatly affected by the offset, which is related to the technological fabrication process, packaging, operating conditions and ageing [11]. Offset is also induced by any mismatch or imbalance in the Hall plate. By definition, the offset is a parasitic voltage that adds to the Hall voltage:

$$V_{out} = V_{HALL} + V_{offset} \tag{8}$$

The current-spinning or connection-commutation technique [11] produces a considerably lower residual offset by an averaging on several phases:

$$V_{offset} = \frac{1}{no.\ of\ phases} \sum_{i=1}^{no.of\ phases} V_i \tag{9}$$

where V_i is the individual phase offset, expressed in volts.

In Figure 10, the 4-phase residual offset is measured three times for three different Square Hall cells, against the biasing current.

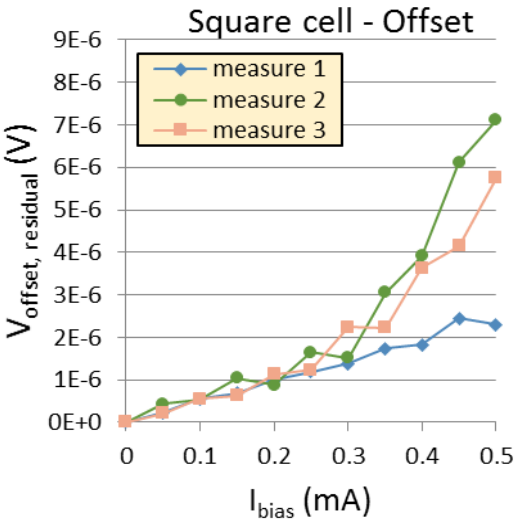

Fig. 10. Measured residual offset *vs.* biasing current, for Square Hall cell

We can see, from Figure 10, that the low offset values for the Square cell do not exceed 7 µV, for a maximum current of 0.5 mA.

C. Summary of experimental results regarding Square Hall cell main parameters

This table summarizes the experimental numerical values of the Square Hall cell main parameters, obtained through the corresponding electrical and magnetic measurements. It is worth mentioning that the value for the absolute sensitivity has been obtained for a biasing current of 1 mA, while the offset drift was obtained for 0.5 mA. Also, a permanent magnet with a magnetic field strength B=0.5 T was used for the sensitivity measurements.

Table 1

Main parameters of the Square Hall cell

Numerical values					
R (kΩ)	***Width W (μm)***	***Length L (μm)***	***Contacts size s***	***Absolute sensitivity S_A (mV/T)***	***Offset drift (μT/°C)***
4.9	20	20	2.3	95.2	0.082

5. Conclusions

The work in this paper was devoted to look into geometrical optimization approaches for Hall cells, with an emphasis on both square and rectangular shapes, with small sensing contacts.

To attain the stated objectives, maximization for the geometrical correction factor was performed, with respect to various imposed technological parameters such area and sensing contacts size. At this point, we have seen that the maximum geometrical correction factor *G* is obtained for maximum area *A* and minimum contacts size *s*.

We have inferred that in order to maximize the sensitivity of Hall cells, within the same technological process, the geometrical correction factor needs to be maximized.

Experimental results for the square Hall cells integrated in a 0.35 μm CMOS technological process have been offered, for both the sensitivity and offset. In order to have a complete overview on the performance of the Hall cells, three-dimensional physical models have been developed for the square Hall cells.

As future work, the authors are planning to extend this analysis to CMOS SOI (Silicon on Insulator) Hall cells, structures already integrated.

Ackowledgements

The first author would like to thank Hasler Foundation, from Switzerland, for awarding the financial support to work on her own project, as principal investigator.

R E F E R E N C E S

[1]. *R.S. Popovic*, Hall Effect Sensors, 2nd ed., Institute of Physics Publishing Bristol and Philadelphia, UK, 2004.
[2]. *E. Ramsden*, Hall-Effect Sensors - Theory and Applications, 2nd ed., Elsevier, United States of America, 2006.
[3]. *X. Larrucea, S. Mergen, A. Walker,* A GSN Approach to SEooC for an Automotive Hall Sensor, Proceedings of the EuroSPI 2016: Systems, Software and Services Process Improvement, pp. 269-280, 2016.
[4]. *A. Manzin, V. Nabaei, O. Kazakova,* Modelling and optimization of submicron Hall sensors for the detection of superparamagnetic beads, Journal of Applied Physics, Vol. **111**, Issue 7, 2012, pp. 1-3, 07E513.
[5]. *B. A. Tuan, A. d. S-Daw, H. M. Phuong, T. M. Hoang, N. T. Dzung*, Magnetic camera for visualizing magnetic fields of home appliances, Proceedings of 2014 IEEE Fifth International Conference on Communications and Electronics (ICCE), 2014.
[6]. *M.A. Paun, J.M. Sallese, M. Kayal,* Evaluation of characteristic parameters for high performance hall cells, Microelectronics, **Vol**. 45, Issue 9, pp. 1194-1201, 2014.
[7]. *M.A. Paun, F. Udrea,* SOI Hall cells design selection using three-dimensional physical simulations, Journal of Magnetism and Magnetic Materials, Vol. **372**, pp. 141-146, 2014.
[8]. *M.A. Paun, J.M. Sallese, M. Kayal*, Temperature considerations on Hall Effect sensors current-related sensitivity behaviour, Analog Integrated Circuits Signal Processing, Vol. **77**, Issue 3, pp. 355-364, Special Issue: SI, 2013.
[9]. *M.A. Paun, J.M. Sallese, M. Kayal*, A Circuit Model for CMOS Hall Cells Performance Evaluation including Temperature Effects, Advances in Condensed Matter Physics, Article ID 968647, 2013.
[10]. *M.A. Paun, J.M. Sallese, M. Kayal,* Geometry influence on the Hall effect devices performance, University Politehnica Of Bucharest Scientific Bulletin-Series A-Applied Mathematics And Physics, Vol. **72**, Issue 4, pp. 257-271, 2010.
[11]. *M.A. Paun,* Hall Cells Offset Analysis and Modeling Approaches, EPFL, Switzerland 2013, PhD Thesis.
[12]. *U. Ausserlechner,* Two Simple Formulae For Hall-Geometry Factor Of Hall-Plates With 90 Degrees Symmetry, University Politehnica Of Bucharest Scientific Bulletin-Series A-Applied Mathematics And Physics, Vol. **78**, Issue 1, pp. 275-282, 2016.
[13]. Synopsys TCAD software tools online documentation, access at the address: ⟨http://www.synopsys.com/Tools/TCAD⟩.